Bull. Mater. Sci., Vol. 34, No. 2, April 2011, pp. 389–399. © Indian Academy of Sciences.

Formation of hydroxyapatite coating on titanium at 200°C through pulsed laser deposition followed by hydrothermal treatment

MANOJ KOMATH[†], P RAJESH[†], C V MURALEEDHARAN[†], H K VARMA[†], R RESHMI and M K JAYARAJ*

Department of Physics, Cochin University of Science and Technology, Kochi 682 022, India
[†]Biomedical Technology Wing, Sree Chitra Tirunal Institute for Medical Sciences and Technology, Trivandrum 695 012, India

MS received 14 November 2008

Abstract. Pulsed laser deposition (PLD) has emerged as an acceptable technique to coat hydroxyapatite on titanium-based permanent implants for the use in orthopedics and dentistry. It requires substrate temperature higher than 400°C to form coatings of good adhesion and crystallinity. As this range of temperatures is likely to affect the bulk mechanical properties of the implant, lowering the substrate temperature during the coating process is crucial for the long-term performance of the implant. In the present study, hydroxyapatite target was ablated using a pulsed Nd:YAG laser (355 nm) onto commercially pure titanium substrates kept at 200°C. The coating thus obtained has been subjected to hydrothermal treatment at 200°C in an alkaline medium. The coatings were analysed using microscratch test, optical profilometry, scanning electron microscopy (SEM), energy dispersive spectroscopy (EDS), X-ray diffraction (XRD) and infrared spectroscopy (FTIR). XRD, EDS and FTIR showed that the as-deposited coating contained amorphous calcium phosphate and the hydrothermal treatment converted it into crystalline hydroxyapatite. The micro-morphology was granular, with an average size of 1 micron. In the microscratch test, a remarkable increase in adhesion with the substrate was seen as a result of the treatment. The plasma plume during the deposition has been analysed using optical emission spectroscopy, which revealed atomic and ionic species of calcium, phosphorous and oxygen. The outcomes demonstrate the possibility of obtaining adherent and crystalline hydroxyapatite on titanium substrate at 200°C through pulsed laser deposition and subsequent hydrothermal treatment.

Keywords. Pulsed laser deposition; hydroxyapatite; hydrothermal treatment; titanium implants; bioactive coatings.

1. Introduction

Titanium and its alloys are used for permanent implants in orthopedics and dentistry. In the case of endosseous screws and joint prostheses, the implant observes heavy mechanical loading, posing a challenge in achieving long-term fixation. Attachment of the implant surface to the host bone is the deciding factor in implant stability. The lack of biological interface with the host bone leads to aseptic loosening, which necessitates revision surgery.

An accepted method for providing bioactive surface for titanium implants is to coat with calcium phosphates (CaP), particularly hydroxyapatite (HA). The CaP materials, owing to their similarity with the mineral content of natural bone, act as an active interface for bony tissue proliferation. It has been demonstrated that CaP coatings provide good apposition with host bone and promote early fixation of the implants by encouraging chemical bonding between new bone and the surface of these materials (Nelea *et al* 2007; Koch *et al* 2007). The clinical advantage of HA coated implants has been established through several studies (Ducheyne *et al* 1990; Klein *et al* 1991; Tisdel *et al* 1994). Various techniques have been reported to apply calcium phosphates coatings on titanium alloys, such as plasma spray, magnetron sputtering, ion beam assisted deposition, chemical vapour deposition, electrophoretic deposition, electrochemical deposition, sol–gel coating, biomimetic coating and pulsed laser deposition (PLD) (Koch *et al* 2007; Nelea *et al* 2007). Typical advantages and shortcomings can be found for all the methods (Ferro *et al* 2005).

Plasma spray is the only commercially available method currently, for coating the implant materials with calcium phosphates, especially with hydroxyapatite (HA) (Koch *et al* 2007; Nelea *et al* 2007). However, the plasma-sprayed HA coatings show certain drawbacks in the final clinical applications, like poor adherence to the metal surface and the lack of uniformity in morphology and crystallinity (Garciýa-Sanz *et al* 1997; Fazan and Marquis 2000).

In the past decade, pulsed laser deposition (PLD) technique emerged as a promising alternative for coating titanium

*Author for correspondence (mkj@cusat.ac.in)

implants with hydroxyapatite (Bao *et al* 2005; Koch *et al* 2007; Nelea *et al* 2007). In this technique, a dense hydroxyapatite target is ablated by an intense pulsed laser (with wavelengths of 355 nm or lower) and the substrate metal is kept in front of the radiating plasma plume to acquire the ablated material over its surface. It has more versatility and controllability as opposed to plasma spray and other techniques. The advantage of PLD technique is the ability to deposit uniform, pure, crystalline and stoichiometric hydroxyapatite films (Mihailescu *et al* 2005).

The deposition process in PLD demands a minimum level of substrate temperature for obtaining phase-pure hydroxyapatite. Though calcium phosphates in general are biocompatible, crystalline hydroxyapatite is preferred for *in vivo* stability (Koch *et al* 2007; Nelea *et al* 2007). Studies over the years have established that it is very difficult to obtain crystalline and adherent hydroxyapatite coatings below a substrate temperature of 400°C (Bao *et al* 2005; Johnson *et al* 2006). Lower temperatures lead to the formation of amorphous calcium phosphates and non-stoichiometric apatites in the coatings. These phases will undergo faster resorption *in vivo* and adversely affect the clinical success of the implant. Depending on the deposition parameters and chamber atmosphere, amorphous calcium phosphate is likely to be formed even at temperatures higher than 400°C, which is attributed to the loss of the hydroxyl ions from the hydroxyapatite crystals (the target material) during the laser ablation process. In order to tackle this problem, depositing the coatings in water vapour atmosphere has been introduced. It has also been identified that post-deposition annealing in water vapour helps in reinstating the hydroxyapatite stoichiometry in the amorphous coating formed at lower deposition temperature (Koch *et al* 2007; Nelea *et al* 2007). However, even in these cases, substrate has to undergo a thermal treatment cycle around 400°C. Though it is established that higher substrate temperatures improve the adhesion and quality of coatings on the surface, the effect of temperature on the bulk of the substrate has not been addressed.

It is well known that a thermal treatment of titanium metal will lead to the absorption of hydrogen, carbon, oxygen and nitrogen from the surrounding atmosphere (Gasser 2001; Davis 2006). These small atoms enter into the metal lattice interstitially and inhibit plastic deformation, thereby causing substantial loss in ductility. The hydrogen embrittlement seems to be most detrimental. The process will become prominent at about 500°C (Davis 2006). It is clear that the processing temperatures, applied in the PLD processing to obtain good hydroxyapatite coatings, are likely to affect the bulk mechanical properties of titanium metal. This, in turn, will reflect adversely in the long-term performance of a permanent implant. The effect may be drastic in the case of endosseous implants and joint prostheses which undergo heavy and dynamic loading.

The present paper describes a pulsed laser deposition (PLD) based method to coat adherent crystalline hydroxyapatite at reduced substrate temperatures so that the bulk mechanical properties of the implant are preserved. The rationale is developed based on the possibility of converting amorphous or non-apatitic calcium phosphates to crystalline hydroxyapatite through hydrothermal treatment at a temperature, of the order of 200°C (Huang *et al* 2000; Jinawath *et al* 2001). In the present experiment, sintered hydroxyapatite target is ablated onto a titanium substrate at 200°C through PLD, anticipating that the coating formed will be amorphous. This is further subjected to hydrothermal treatment in alkaline medium. Parameters of temperature, treatment time, process pH etc are optimized through testing the coating adhesion and phase conversion. Throughout the process steps, the maximum temperature has been limited to 200°C.

2. Experimental

2.1 *The set up*

The deposition had been done in a custom designed spherical chamber which contained target and substrate holders facing each other, along with laser focusing lens assembly and gas inlet port. Additional windows/ports were provided for optical emission analysis etc. The target holder can carry multiple targets, each of which could be rotated eccentrically (for uniform erosion) using externally mounted motor and gears. The substrate holder was integrated onto a concealed heater with a shutter in the front. An external PID controller powered the heater so that the substrate temperature could be maintained at the required value. A side window (at 135° angle from the target holder port) was used to mount the focusing assembly for the laser beam. A schematic layout of the pulsed laser deposition system is given in figure 1. The target selection, rotation, shutter position and laser beam were controlled using a microprocessor-based remote control unit.

2.2 *Deposition procedure*

The targets were made out of 99·99% pure hydroxyapatite (125 micron grade, prepared in-house) by compressing to 800 bar in cold isostatic press and sintering at 1100°C for 2 h. This helped to achieve a density above 3. They were ground to disc shape and mounted on the target holder.

A Nd:YAG (neodymium doped yttrium aluminum garnet) pulsed laser (Quanta Ray, Spectra Physics) operating at 355 nm, 10 Hz repetition rate, was used for the ablation. The laser beam was focused onto the target using a quartz lens ($f = 30$ cm) at an angle of 45° with respect to the target normal and the spot size was adjusted to 2 mm diameter. The target and chamber were kept at ground potential.

Commercially pure titanium (cp-Ti) discs of 20 mm diameter and 1 mm thickness were used as substrates. The surface intended for coating has been subjected to progressive polishing with carbide grits of diminishing size grades,

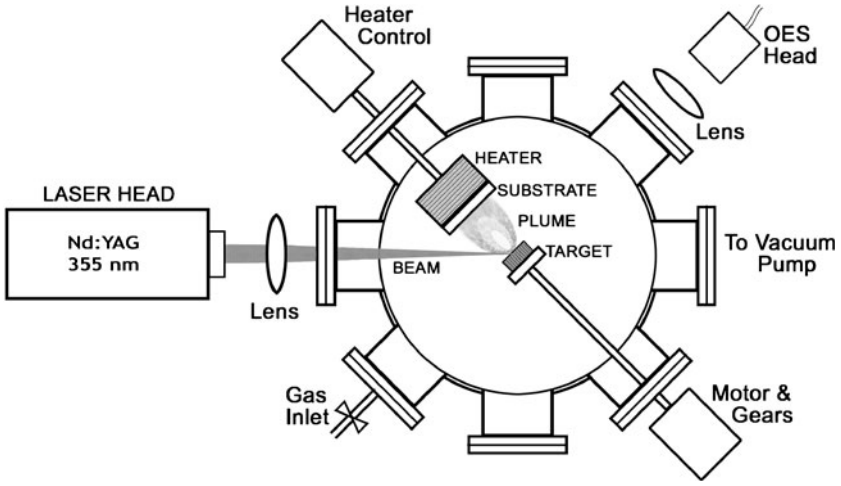

Figure 1. Schematic of deposition system.

and finally with 0·05 micron diamond paste. Surface profilometry gave the roughness values after the final step to be 0·025 microns. The polished discs were then cleaned in ultrasonic bath, dried and mounted onto the substrate holder. The target-substrate distance was adjusted to 4 cm and the shutter was kept closed.

The chamber was pumped down to a pressure of 10^{-5} mbar by means of a diffusion pump backed by rotary pump. After stabilizing at the base pressure, pure, dry nitrogen gas was admitted via a mass flow controller, to bring the pressure to $\sim 10^{-3}$ mbars. The substrate was kept stable at 200°C before deposition. The laser power was adjusted so as to obtain a fluence of 3 J/cm^2. The opening and closure of the shutter in front of the substrate marked the time of deposition.

The coatings were deposited for a period of 2 h. In the case of samples for thickness measurements, surface masking was done up to the middle portion. The coated substrates were taken out after cooling down. Two sets of samples were prepared, one for analyzing as-deposited and the other for hydrothermal treatment.

2.3 *Post-deposition treatment*

The hydrothermal treatment of the coatings was done in a Teflon-lined stainless steel autoclave. Ammonium hydroxide solution of pH 8·5 was used as the medium. The temperature was maintained at 200°C for 8 h, without stirring. The pressure developed was measured to be 0·2 MPa.

2.4 *Thickness measurements*

The thickness had been measured using Dektak 6M contact surface profiler, which electromechanically records the step-height at a discontinuity. The sample was moved beneath the diamond tipped stylus of the instrument so that the masked edge of the coating came across the path. The sample travel length was 200 microns with a stylus force of 4 mg.

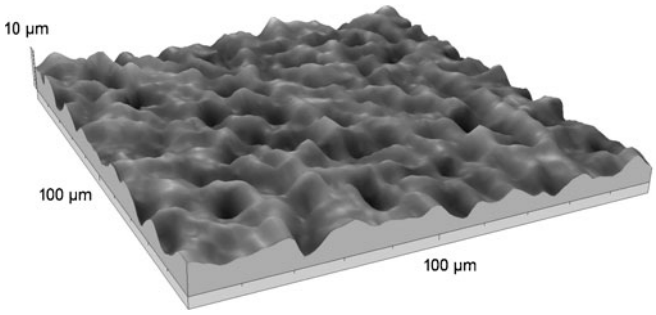

Figure 2. The surface profile of the as-deposited coating obtained through Talysurf CLI 1000.

2.5 *Surface imaging*

Surface image analysis of the as-deposited sample was done through non-contact surface profilometry with Talysurf CLI 1000 (Taylor Hobson) 3D Profiling System. Chromatic length aberration (CLA) gauge has been used, which works under 'confocal' principle and offer high resolution 3D measurement of the surface (Garzón *et al* 2004). It consisted of a white light source, a spectral aberration lens extended with optical fibre cable and an optical analysis system with pinhole, grating and CCD sensor. The spectral aberration lens projects white light onto the sample surface. The chromatic aberration causes spectral dispersion and at any point on the surface, only a certain wavelength will be in focus. The spectral image reflected from the surface was collected by the same lens and optic cable and passed into the optical analyser with the help of a beam splitter. The pin hole and grating in the analyser permits only the wavelength in focus to pass through and the CCD sensor interpolates the spatial position of the data point.

The sample was moved in X, Y and Z axes using a high precision motorized stage and data was collected one point at a time. CLA 300 gauge (range 300 μm and resolution 10 nm) was selected. The measurement was done at a speed of 200 μm/s with a sampling rate of 200 Hz, in an XY envelope of 100 μm length with 1 μm spacing. The Z axis measurement of the CLA gauge was calibrated using a secondary roughness standard (traceable to United Kingdom Accreditation Service–UKAS) and is capable of providing a measurement uncertainty of ±25 nm.

2.6 *Micro scratch test*

Adhesion studies on the coatings were carried out using micro-scratch method. The technique involves generating a controlled scratch with a diamond tip on the coating surface under either constant or progressive load. Acoustic, friction and tip position data are collected by appropriate sensors attached to the indenter holder. The failures of the coating under the loading, corresponding to different mechanisms, manifest as sudden changes in friction and acoustic emission. The load values at the initiation of these failures (first crack, first delamination and total delamination) are defined as critical loads (Lc), which quantify the adhesive properties of the coating on the given substrate.

The test had been performed in a micro-scratch test system (Micro-Combi Tester, M/s CSM Instruments, USA). A linearly progressive normal load was applied with a Rockwell (Diamond) indenter of 100 μm radius. The test parameters were fixed to those values which give reproducible scratch maps. The starting load was 0·05 N (default value) with a loading rate 25 N/min. The final load and scratch length were selected so that total delamination occurs within the scratch span. Testing was performed over a scratch length of 6 mm at a speed of 10 mm/min, with a final load value of 15 N. The critical loads for first crack event (Lc1), first delamination (Lc2) and total delamination (Lc3) were determined from the data. As the friction values may fluctuate due to the presence of particle debri and local irregularities, the critical loads were reconfirmed using the acoustic data. The failure events were verified using the penetration depth profile as well as with the help of optical microscopy.

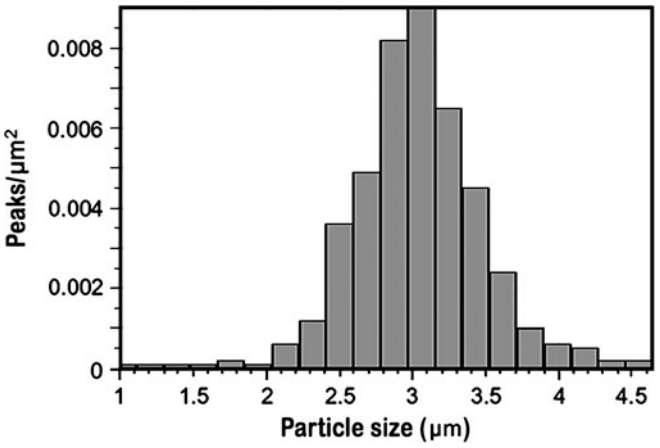

Figure 3. Peak count histogram corresponding to figure 2.

2.7 *Scanning electron microscopy and energy dispersive analysis*

Scanning electron micrographs of the samples were taken in Quanta ESEM (environmental scanning electron microscope from FEI) in low vacuum mode, without gold coating over the surface. An attached energy dispersive analyser (EDAX) has been used for determining the calcium-to-phosphorous ratio.

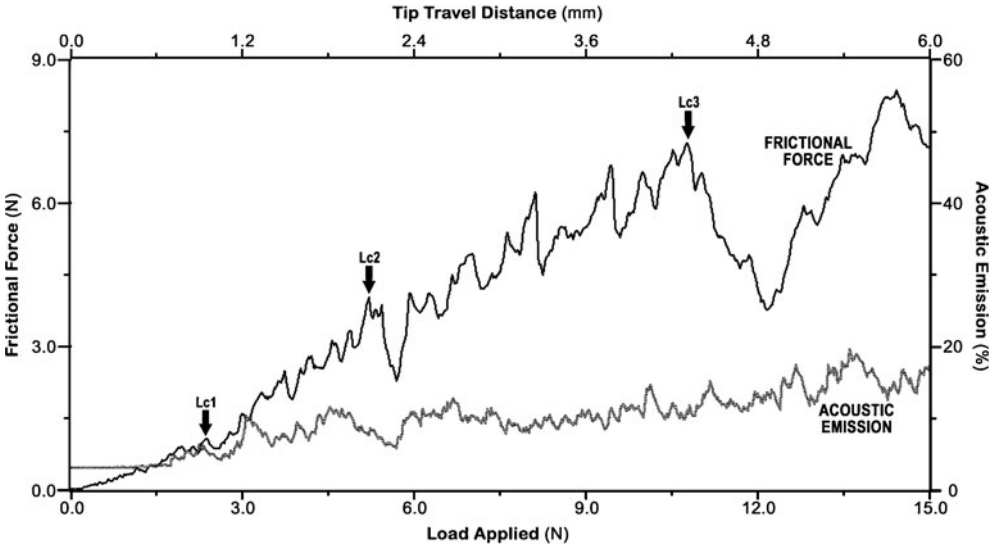

Figure 4. Results of micro-scratch test done on as-deposited sample.

2.8 *X-ray diffraction studies*

Phases of the materials in the coating were analysed using X-ray diffraction (XRD–Rigaku DmaxC model) with CuKα radiation ($\lambda = 1{\cdot}5418$ Å). The scanning was done in θ–2θ mode in the range of 10–50° with a fixed incident angle of 1°.

2.9 *Infrared spectroscopy*

Infrared spectra of the coatings were taken in a Thermo-Nicolet 5700 FTIR spectrophotometer, with KBr beam splitter and deuterated lanthanum triglycerine sulphate (DLaTGS) detector. As the samples were in the form of coatings on a surface, a specular reflectance attachment (30Spec, PIKE Technologies) was used. This attachment, when fitted in the sample compartment, directed the infrared beam onto the sample surface at 30° angle and the reflected part was passed into the detector with the help of mirrors. The spectrometer was set to collect 100 scans on samples in the range 500–4000 cm^{-1} at a resolution of 4 cm^{-1} and the final spectra was constituted by subtracting the background (64 scans).

The infrared spectra of both the as-deposited and processes coatings were taken in specular reflectance mode. Also, the spectrum of the hydroxyapatite target (on the surface of the pellet) was taken for comparison.

2.10 *Optical analysis of plume*

An attempt had been made to identify the various species present in the ablation plume. Triax 320 compact imaging spectrometer (Horiba Jobin Yvon) was used to analyse the emission wavelengths of the atomic and ionic species present in the luminous plume emanating from the target surface.

The side window of the chamber (at 90° angle from the target holder port, as shown in figure 1) had been utilized for optical analysis. The image was focused using a convex quartz lens of focal length 50 mm onto an optic fibre head mounted on a micrometer stage. The stage enabled linear translation motion of the head along the axis of the image of the plume. The optical fibre cable extended to the spectrometer to couple optically to the entrance slit of the monochromator (grating with 1200 grooves/mm). The wavelength-dispersed spectrum of the plume was collected using a charged coupled device (SpectrumOne-2000 CCD, 1024 × 256 pixels). The real-time data during the ablation process was ensured by triggering the CCD externally using voltage pulses from the laser controller. The data were stored in a personal computer interfaced with the spectrometer for subsequent processing.

Before the measurements, the resolution ($\Delta\lambda$) of the spectrometer had been determined by directing the fibre optic head towards a mercury lamp and analysing the two emission lines at 578·88 and 576·75 nm (Joshy *et al* 2008). The resolution of the spectrometer turned out to be 0·064 nm. The measurements were done along the propagation direction of the plume after it got stabilized. Emission spectra were collected in the wavelength range 390–700 nm at an interval of 1 mm, in the distance range of 5–15 mm from the target surface. The emissions very close to the target (<5 mm) contained high noise levels and at distances larger than 15 mm, but the intensities were very poor.

3. Results

The pulsed laser deposition of hydroxyapatite target on cp-Ti substrate resulted in a continuous whitish coating. The step thickness obtained through surface profilometry on a coating

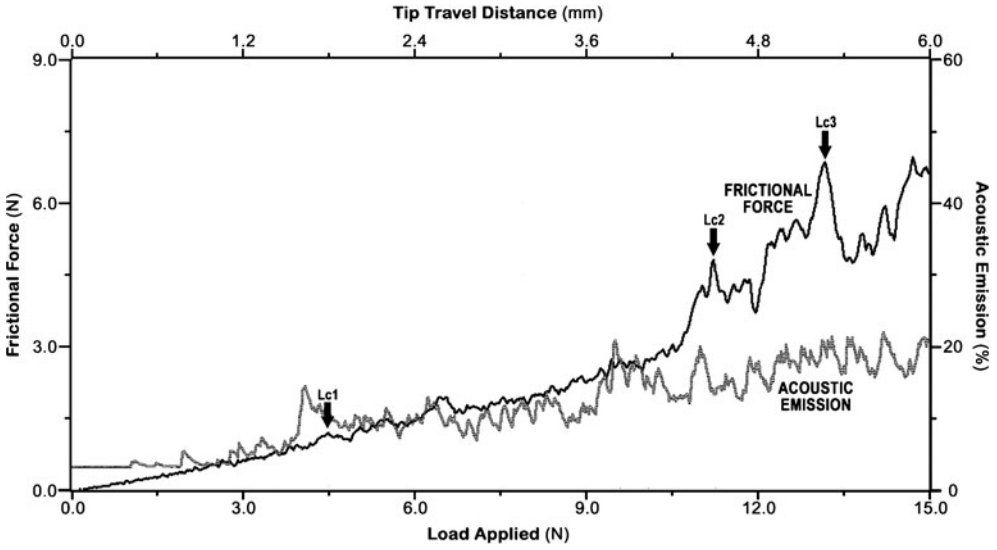

Figure 5. Results of micro-scratch test done on hydrothermally treated sample.

done for 2 h was 7·92 microns, giving the deposition rate to be 3·96 microns per hour.

In scanning electron microscopy, the as-deposited coating appeared to be composed of globules of a few microns size, with snowy appearance and remarkable uniformity. The surface microstructure did not reveal any crystalline growth features. The 3D surface profile obtained in the Talysurf CLI 1000 also showed distribution of globules (figure 2). An estimate of the globule sizes could be obtained from the peak-count histogram (figure 3) associated with the surface profile data. The size distribution ranged from 2 microns to 4·3 microns, which is centred around 3 microns.

Figures 4 and 5 represent the results of the micro-scratch tests done on the as-deposited and hydrothermally treated samples, respectively. The graphs corresponding to frictional force (bold trace) and acoustic emission (shaded trace) for a tip travel distance of 6 mm with 15 N load, with the same test parameters, are given in each case. The critical loads for first crack (Lc1), first delamination (Lc2) and total delamination (Lc3) are marked.

The frictional force data of the as-deposited coating shows very high fluctuation, indicating the flaking-off of the material onto the scratch path. This is a mark of low cohesiveness of the coating. On the other hand, the frictional force on the treated coating shows almost a uniform increase till the delamination stage. This is an indication of uniform, dense coating. The critical load values obtained in both cases are compared in table 1.

The scanning electron micrograph of the hydrothermally treated sample subjected to scratch test (corresponding to figure 5) is given in figure 6. The focused area is at the first crack (Lc1). It can be seen that the indenter tip has ploughed through the coating showing that the inter-particulate bonding is not stronger. The scratch tip has intended the underlying metal, yet the material has not been detached.

A magnified view of the surface of the same (hydrothermally treated) sample can be seen in figure 7. The particle sizes are uniform except for the local agglomeration at some points. The size distribution is in the range 0·8–1·5 microns, less than that of the globules observed in the as-deposited sample (figures 2 and 3). The average particle size, measured in SEM, is 1 micron.

The X-ray diffraction spectra of as-deposited and hydrothermally treated calcium phosphate coatings in the 2-Theta range 10–50° are given in figure 8 (in the top panels). The standard hydroxyapatite diffraction lines (JCPDS Data Card 09-0432 1996) are represented by the bottom panel.

Due to the grazing angle configuration, the intensities were low, resulting in a noisy spectrum. The strong peaks observed at 2-theta angles 35·1, 38·45 and 40·15 (marked with asterisk in both the traces) correspond to metallic titanium, the substrate material (JCPDS Data Card 44-1294). The remaining

Table 1. Critical loads determined from the micro-scratch test data on the calcium phosphate coatings on titanium surface, as-deposited and hydrothermally treated.

	Critical loads (N)	
Parameter	As-deposited	Hydrothermally treated
First crack (Lc1)	2·35	4·44
First delamination (Lc2)	5·42	11·25
Total delamination (Lc3)	10·77	13·16

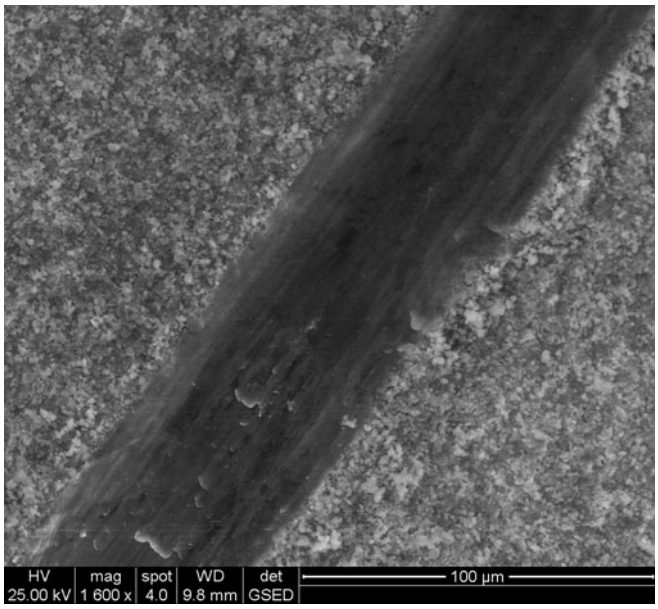

Figure 6. Scanning electron micrograph of scratch track corresponding to figure 5, at position of Lc1.

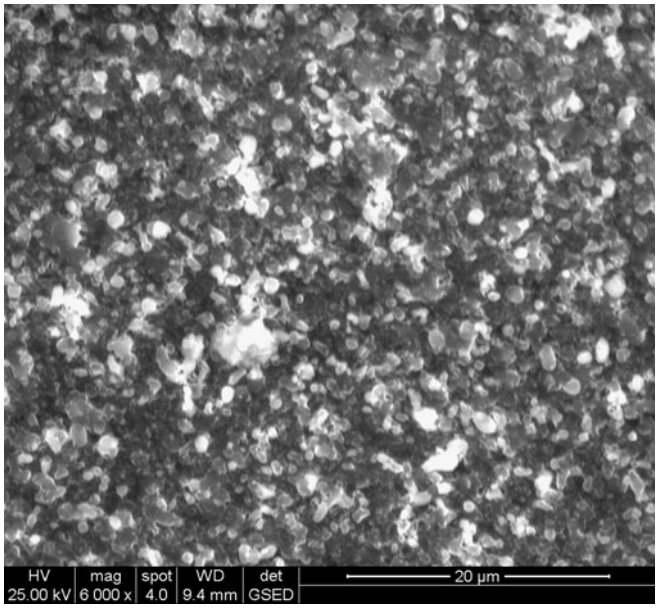

Figure 7. A magnified view of coating surface of hydrothermally treated sample.

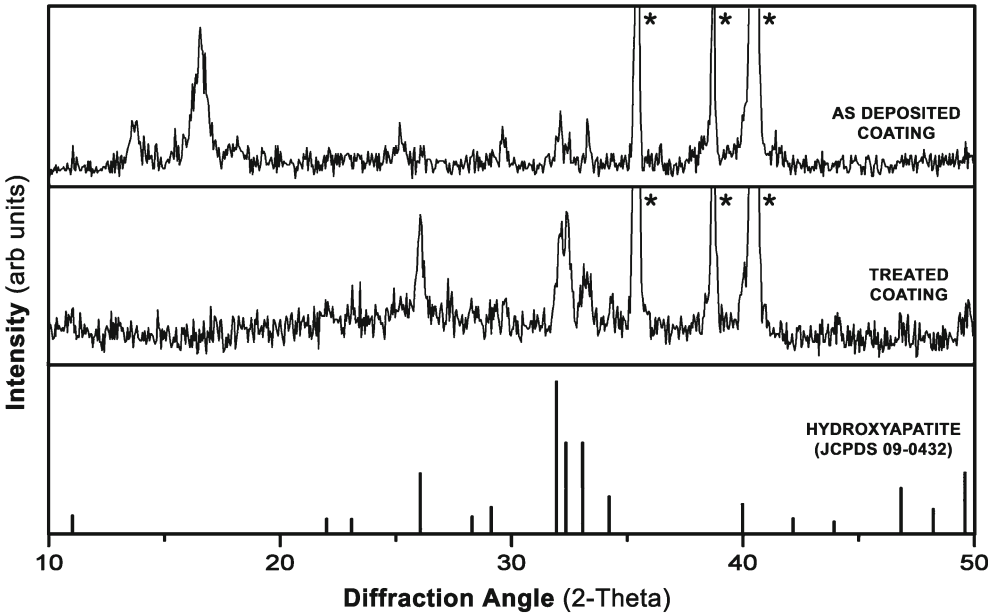

Figure 8. X-ray diffraction spectra of as-deposited (top panel) and hydrothermally treated (middle panel) coatings. Standard diffraction lines of hydroxyapatite are given in bottom panel for comparison.

peaks in the traces were compared with the diffraction data corresponding to the various calcium phosphate phases available in the JCPDS files. The change of phase composition of the coating after the hydrothermal treatment is evident. The various peaks in the trace match well with the standard hydroxyapatite diffraction lines.

The distinct peaks at 2-theta angles 13·5, 16·3, 25·2 and 29·5 in the as-deposited sample did not match with the lines of any of the calcium phosphate phases, within the error limit. However, the distribution (position and intensity) resembled the data (JCPDS Data Card 44-0761) for calcium pyrophosphate ($Ca_2P_2O_7{\cdot}2H_2O$, monoclinic). The broadening of the peaks indicates low crystallinity of the material. Some feeble peaks were present at the positions of strong lines of hydroxyapatite.

The energy dispersive analysis (EDS) of the as-deposited and treated coatings showed that both have nearly the same Ca–P ratio (1·62), which is close to that of the target material (1·67). The EDS spectrum of the treated coating is given in figure 9. It carries the information corresponding to titanium substrate also, because of the low thickness of the coating.

Figure 10 represents the FTIR spectra of the samples, in the wave number range 1200–500 cm^{-1} which covers the bending and stretching absorption regions of calcium phosphates. The FTIR spectrum of the as-deposited sample is given as trace **a**. The changes after hydrothermal treatment could be seen in trace **b**. For comparison, the spectrum of hydroxyapatite target also is given (trace **c**). The inset contains part of the spectrum in the wave number range 3630–3500 cm^{-1}. This region helps to confirm the characteristic OH peak of hydroxyapatite specifically, reported to be at 3570 cm^{-1} (Zeng and Lacefield 2000). The values marked

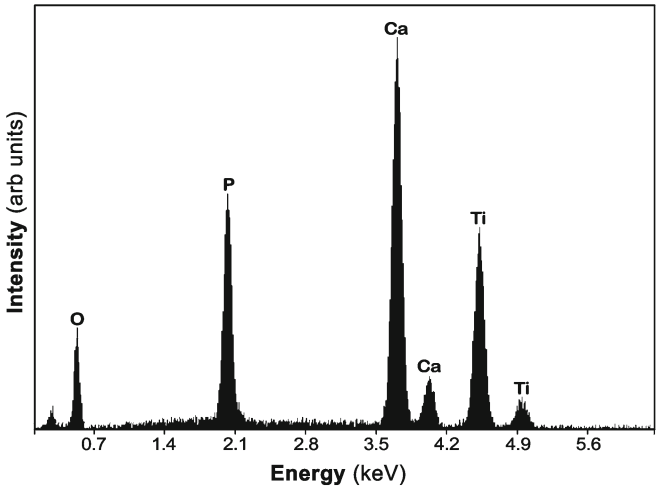

Figure 9. Energy dispersive spectrum of sample.

in the traces are those corresponding to the crest of the peak or band.

The notable feature of the spectrum of the as-deposited sample is the prominent peak at 1012 cm^{-1}. Small shoulder peaks at 961, 1085 and 1114 cm^{-1} are observed. The bands corresponding to PO bending (centred at 563 and 599 cm^{-1}) and that corresponding to OH group (centred at 3565 cm^{-1}) are weak. In the hydrothermally treated sample, all the peaks corresponding to hydroxyapatite (573, 602, 630, 963, 1055, 1088 cm^{-1}) appeared (Pleshko *et al* 1991; Soten *et al* 1999). The target material gave a typical spectrum corresponding to hydroxyapatite. On comparison with the spectrum obtained for the treated coating, the peaks of the target material were

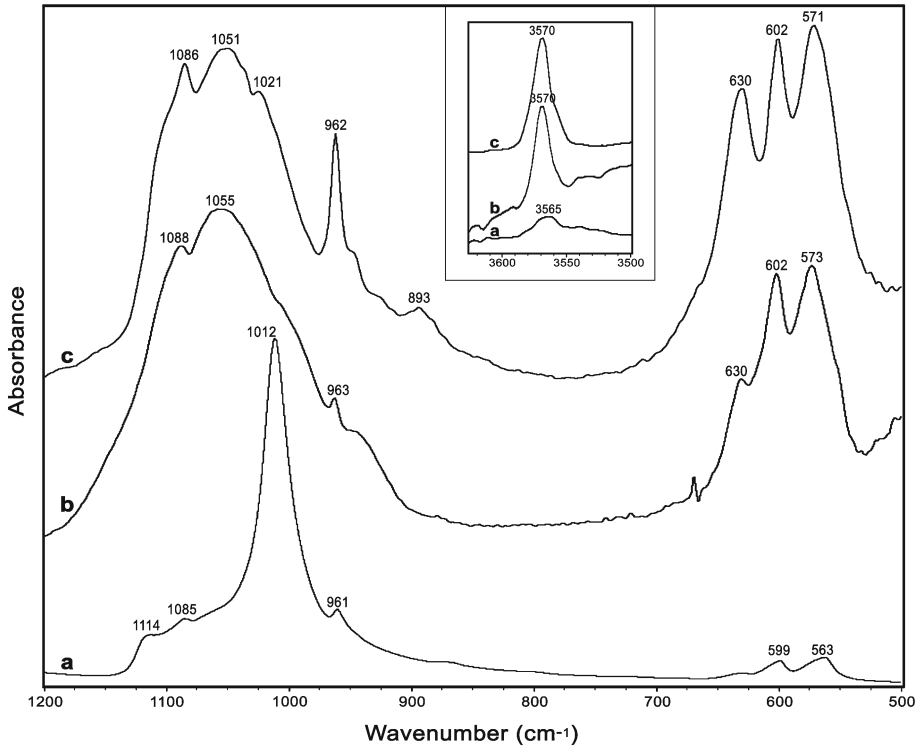

Figure 10. FTIR spectra of samples corresponding to bending and stretching regions of calcium phosphates. Traces **a** and **b** correspond to as-deposited and hydrothermally treated samples, respectively. Trace **c** is that of target material. Inset corresponds to region of hydroxyl bands in calcium phosphates.

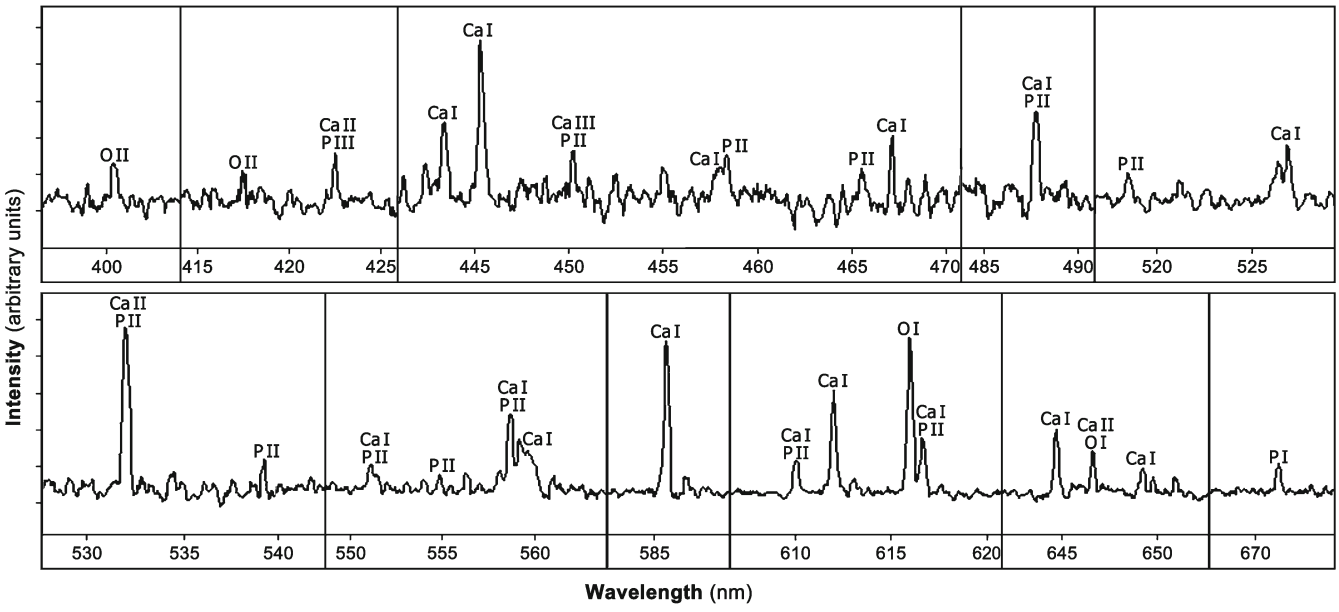

Figure 11. Optical emission spectra of laser ablation plume at 15 mm from target plane.

stronger and more resolved, especially those at 630, 962, 1021 and 1086 cm^{-1}. Both the treated sample and target material showed peaks at 3570 cm^{-1} corresponding to the lattice hydroxyl group (Zeng and Lacefield 2000).

Emission spectra from the plume in the range 390–700 nm were recorded at distances from 5 mm to 15 mm from the target surface, 1 mm apart. These did not vary regarding the peak positions and intensities. The selected parts of the

spectrum at a distance of 15 mm from the target surface are given in figure 11.

Prominent peaks are selected and interpreted using the atomic spectra database of NIST, version 3·1·4 (NIST URL http://physics.nist.gov/asd3). The spectrum is found to consist mainly of emission lines of calcium, phosphorous and oxygen. The emission from calcium is dominated by atomic (Ca I) species, which is in agreement with the data reported (Niemz 1994; Serra and Morenza 1998; Mroz *et al* 2007). Ionic lines (Ca II and Ca III) are also present. The emissions from phosphorous and oxygen appear in the spectra, which were reported to be difficult to observe by other workers.

In the case of phosphorous, ionic lines (P-II) are prominent, whereas P-I and P-III emissions are feeble. Oxygen emissions are mainly from atomic species (O-I). Ionic oxygen species (O-II) is also seen in low quantities, which is rarely reported. The presence of phosphorous and oxygen lines may be due to the higher laser fluence provided in the experiment. Though many of the lines are seen superimposed, there is not much ambiguity in interpretation because supporting emission lines are present. The optical emission analysis of the plume revealed a typical hydroxyapatite ablation process.

4. Discussion

The present experiment is an attempt to deposit hydroxyapatite on titanium substrate through pulsed laser technique at a temperature of 200°C, much lower than the conventionally applied range. Water vapour is not used in the chamber for two reasons: (i) water vapour was not found useful in producing the required phase at this temperature, and (ii) hydrothermal post-treatment in aqueous medium is envisaged in the method. The deposition rate measured is 3·96 microns per hour which translates to 1·1Å per laser pulse. This rate is on the higher side of that obtainable with the 3rd harmonic of Nd:YAG lasers ($\lambda = 355$ nm) (Koch *et al* 2007).

Two kinds of ablation mechanisms are involved in the pulsed laser deposition of calcium phosphate coatings on titanium from a hydroxyapatite target. The first one is the ejection of target material in the form of micrometer-sized particulates and making them adhere to the substrate surface. The second one is the conversion of target material to atoms, molecules and small clusters and allowing them to migrate over the substrate surface to nucleate and grow as crystallites (Fernandez-Pradas *et al* 1999). The optical emission studies indicate that the latter mechanism dominates in the present deposition experiment, as the atomic and ionic emissions of calcium, phosphorous and oxygen are present in the spectrum. The formation of amorphous calcium phosphate could be anticipated as the chamber environment and the substrate temperature are not favourable for the nucleation and growth of hydroxyapatite (Koch *et al* 2007; Nelea *et al* 2007). The deposited material is found slightly calcium-deficient, with a Ca/P ratio of 1·62.

The as-deposited coating appeared amorphous in XRD, with broad (but prominent) humps between 12 and 18° 2-theta angles. However, it was difficult to decipher the identity of the calcium phosphate phase from the data. Though the broad peaks are centred at certain regions, they do not correspond to any of the reported calcium phosphate phases. Further structural information about the material could be extracted from the FTIR analysis.

The infrared absorption spectrum of the as-deposited calcium phosphate coating (trace **a** in figure 10) contains a major peak at 1012 cm^{-1} corresponding to ν_3 stretching of PO_4. The absorption bands at 1051 and 1086 cm^{-1} seen in the spectrum of the target material (given in trace **c**) are not prominent in it and a remnant peak at 1114 cm^{-1} got revealed. Exactly resembling FTIR spectra of PLD calcium phosphate coatings were reported by Zeng and Lacefield (2000), but without any specific comment on it. The reduction in the region 1050–1100 cm^{-1} indicates the absence of HPO_4^{2-} groups (Soten *et al* 1999). Also the spectrum of the as-deposited material lacks the characteristic peaks of hydroxyapatite at 631 and 3570 cm^{-1} corresponding to the hydroxyl group (Zeng and Lacefield 2000). The ν_4 bending region of PO_4 records two weak, broad-bands showing a lack of crystalline symmetry to lift the degeneracy. Thus the FTIR results show that the as-deposited coating is composed of an amorphous composition of calcium phosphate without hydroxyl group in it, which is well in agreement with the XRD data.

The X-ray diffraction spectrum of the as-deposited sample (top panel in figure 8), on closer examination, reveals feeble peaks corresponding to strong lines of hydroxyapatite. It indicates that a fraction of the material exists in hydroxyapatite phase. However, the quantity of the hydroxyapatite phase present could not be further analysed, because of the background noise.

The phase conversion of the as-deposited material to crystalline hydroxyapatite during the hydrothermal treatment is getting unambiguously established by the XRD spectra (figure 8). The broadening of the diffraction peaks of the treated sample may be due to the low particle sizes (in the range of 0·8–1·5 microns). It is notable that the peak at 25·9° 2-theta is stronger than the standard hydroxyapatite peak at the corresponding position. This indicates a preferred orientation for the newly grown crystals in (002) plane.

The FTIR spectrum of the treated sample matches well with that of the target material which contains all the typical absorption bands of hydroxyapatite (Pleshko *et al* 1991; Soten *et al* 1999). The peaks corresponding to antisymmetric ν_4 bending (at 571 and 602 cm^{-1}), symmetric ν_1 stretching (at 962 cm^{-1}) and antisymmetric ν_3 stretching (at 1051 and 1086 cm^{-1}) modes of PO_4^{3-} ions are present. The characteristic peaks of hydroxyl group are seen at 631 and 3570 cm^{-1}. It is generally observed that non-stoichiometric content gives rise to additional peaks, because the presence of HPO_4^{2-} groups and vacancies distort the pattern of P–O stretching modes (Soten *et al* 1999). Such additional peaks or

artifacts are absent in the spectrum of the hydrothermally treated coating. This observation, together with the XRD and EDS analysis, leads to the conclusion that the phase content is calcium-deficient hydroxyapatite.

The role of hydrothermal conditions in growing hydroxyapatite out of amorphous calcium phosphate, has already been discussed (Huang *et al* 2000; Jinawath *et al* 2001). Aqueous alkaline conditions prevailed in the autoclave and there was no significant change in the Ca/P ratio in the resultant material. Therefore, it could be assumed that the treatment caused local dissolution of the amorphous calcium phosphate and the subsequent nucleation and growth of hydroxyapatite onto the titanium surface. The scanning electron micrograph (figure 7) shows a granular morphology which is typical of HA coatings deposited with a Nd:YAG laser at 355 nm in water vapour atmosphere (Fernandez-Pradas *et al* 2000). The particles, which are of remarkably uniform size around 1 micron, lacked growth features when viewed at higher magnification.

The enhancing effect of the hydrothermal treatment on the adhesion of the coating to the substrate is evident from the micro-scratch test results (table 1). There is notable increase in the values of the critical loads for the first crack (Lc1) and total delamination (Lc3). The increase of the load for the first delamination (Lc2) in the treated coating is dramatic, showing increased adhesion. It is reported that amorphous calcium phosphate coatings fail due to forward lateral flaking mechanism, showing adhesive failure. Crystalline coatings are observed to be more adherent to titanium substrate. Among them, crystals grown in granular morphology are generally resisting delamination than the columnar morphology (Cleries *et al* 2000). The scanning electron micrograph of the scratch track (figure 6) does not show any cracking or flaking. The granular structure of the coating might have helped in accommodating the residual stresses. This may be the prime reason for the increase in the critical loads. Also, there is a chance of the titanium-coating interface being modified during the hydrothermal treatment.

The effect of water treatment on the apatite-forming ability of titanium metal surface has been studied in detail by Uchida *et al* (2002). Favourable effects on nucleation of apatitic calcium phosphate on the treated surface have been observed in treatments at 80°C for 24 h at ambient pressures. They indicated that the formation of titania (Ti–OH) gel at the surface due to the presence of hydronium ions, is capable of inducing apatite nucleation. This mechanism could be extended to the present experiment also. During hydrothermal treatment, Ti–OH gel layer might have formed at the interface. The layer might have provided nucleation sites for the dissolved calcium phosphate to grow as crystalline hydroxyapatite. This mechanism explains both the granular structure as well as the enhancement in adhesion, in the treated coating.

The role of the temperature in the nucleation and growth of apatites has also been addressed by others. In a post-deposition annealing study of calcium phosphate coatings with PLD, the transition from amorphous phase to crystalline phase was seen to occur at 340°C (Koch *et al* 2007). It was suggested in the work that post-deposition annealing of hydroxyapatite thin films may be performed at much lower temperatures than have been previously described in the literature. The present study proves that the hydrothermal treatment subsequent to PLD can further reduce the temperature of the amorphous-to-crystalline transition of hydroxyapatite, to a value of 200°C.

5. Conclusions

The present work demonstrates a new method to obtain crystalline and adherent hydroxyapatite coating over titanium substrate at 200°C. A dense hydroxyapatite target is ablated in a chamber at $\sim 10^{-3}$ mbars pressures in dry nitrogen atmosphere using pulsed laser. Nd:YAG laser beam of wavelength 355 nm, pulsed at 10 Hz, was used for ablation at a fluence of 3 J/cm^2. Coating is formed on a clean titanium substrate kept at 200°C. The coated substrate has been subjected to hydrothermal treatment at 200°C in an alkaline medium.

The structural analysis using XRD, EDS and FTIR showed the as-deposited material to be amorphous calcium phosphate and the hydrothermally treated coating to be crystalline hydroxyapatite (calcium-deficient apatite). It has also been proved that the hydrothermal treatment enhances the adhesion of the coating to the substrate significantly.

This method is apparently attractive for producing bioactive apatite coatings on titanium, as the current methods involve processing temperatures higher than 400°C. The higher temperatures pose the risk of degradation of mechanical properties of the bulk titanium, making it less reliable for load-bearing implant applications. The temperatures in the present method do not cross 200°C, thereby minimizing the threat of degradation of the mechanical performance. This could be considered as a remarkable step in the explorations for producing crystalline and adherent hydroxyapatite coating over permanent implants in orthopedics and dentistry.

References

Bao Q, Chen C, Wang D, Ji Q and Lei T 2005 *Appl. Surf. Sci.* **252** 1538

Cleries L, Martinez E, Fernandez-Pradas J M, Sardin G, Esteve J and Morenza J L 2000 *Biomaterials* **2** 967

Davis J R 2006 *Corrosion of weldments* (Materials Park, OH: ASM International) p. 158

Ducheyne P, Breight J, Cuckler J, Evans B and Radin S 1990 *Biomaterials* **11** 531

Fazan F and Marquis P M 2000 *J. Mater. Sci. Mater. Med.* **11** 787

Fernandez-Pradas J M, Arias J L, Martinez E, Sardin G and Morenza J L 2000 *Appl. Phys.* **A71** 37

Fernandez-Pradas J M, Cleries L, Sardin G and Morenza J L 1999 *J. Mater. Res.* **14** 4715

Ferro D, Barinov S M, Rau J V, Teghil R and Latini A 2005 *Biomaterials* **26** 805

Garciýa-Sanz F J, Mayor M B, Arias J L, Pou J, Leon B and Perez-Amor M 1997 *J. Mater. Sci. Mater. Med.* **8** 861

Garzón R J, Meneses J, Tribillon G, Gharbi T and Plata A 2004 *J. Opt. A: Pure Appl. Opt.* **6** 544

Gasser B 2001 in *Design and engineering criteria for titanium devices, in Titanium in medicine* (eds) D M Brunette *et al* (Berlin: Springer-Verlag) p. 673

Huang L Y, Xu K W and Lu J 2000 *J. Mater. Sci. Mater. M.* **11** 667

JCPDS Data Cards 1996 (Pennsylvania: International Centre for Diffraction Data)

Jinawath S, Pongkao D, Suchanek W and Yoshimura M 2001 *Int. J. Inorg. Mater.* **3** 997

Johnson S, Haluska M, Narayan R J and Snyder R L 2006 *Mater. Sci. Eng.* **C26** 1312

Joshy N V, Saji K J and Jayaraj M K 2008 *J. Appl. Phys.* **104** 553307

Klein C, Pratka P, van der Lubbe H B, Wolke J G and de Groot K 1991 *J. Biomed. Mater. Res.* **25** 53

Koch C F, Johnson S, Kumar D, Jelinek M, Chrisey D B, Doraiswamy A, Jin C, Narayan R J and Mihailescu I N 2007 *Mater. Sci. Eng.* **C27** 484

Mihailescu I N, Torricelli P, Bigi A, Mayer I, Iliescu M, Werckmann J, Socol G, Miroiu F, Cuisinier F, Elkaim R and Hildebrand G 2005 *Appl. Surf. Sci.* **248** 344

Mroz W, Jedynski M, Hoffman J, Jelinek M, Major B, Prokopiuk A and Szymanski Z 2007 *J. Phys.: Conf. Series* **59** 720

Nelea V, Mihailescu I N and Jelinec M 2007 in *Pulsed laser deposition of thin films* (ed.) R Eason (New Jersey: John Wiley & Sons) p. 421

Niemz M H 1994 *Appl. Phys.* **B58** 273

NIST Atomic Spectra Database (National Institute of Standards and Technology, Gaithersburg, MD) on line at http://physics.nist.gov/asd3 (accessed on September 20, 2008)

Pleshko N, Boskey A and Mendelsohn R 1991 *Biophys. J.* **60** 786

Serra P and Morenza J L 1998 *J. Mater. Res.* **13** 1132

Soten I, Vrey G and Ozin A 1999 *J. Mater. Chem.* **9** 703

Tisdel C L, Golberg V M, Parr J A, Bensuan J S, Staikoff L S and Stevenson S 1994 *J. Bone Joint Surg. Am.* **76** 159

Uchida M, Kim H M, Kokubo T, Fujibayashi S and Nakamura T 2002 *J. Biomed. Mater. Res. (Appl. Biomater.)* **63** 522

Zeng H and Lacefield W R 2000 *Biomaterials* **21** 23